Theoretical Studies of the Isoprene Ozonolysis under Tropospheric Conditions. 2. Unimolecular and Water-Assisted Decomposition of the α-Hydroxy Hydroperoxides

ARTICLE *in* THE JOURNAL OF PHYSICAL CHEMISTRY A · JULY 2003

Impact Factor: 2.69 · DOI: 10.1021/jp034203w

Theoretical Studies of the Isoprene Ozonolysis under Tropospheric Conditions. 2. Unimolecular and Water-Assisted Decomposition of the α-Hydroxy Hydroperoxides

P. Aplincourt[†,‡] and J. M. Anglada*[,†]

Departament de Química Orgànica Biològica, Institut d'Investigacions Químiques i Ambientals de Barcelona, IIQAB-CSIC, c/ Jordi Girona 18, E-08034 Barcelona, Catalunya, Spain, and Laboratoire de Chimie Théorique et Matériaux Hybrides, Ecole Normale Supérieure de Lyon, 46 allée d'Italie, F-69364 Lyon Cedex 07, France

Received: January 24, 2003; In Final Form: April 30, 2003

Theoretical studies of the unimolecular and water-assisted decomposition reactions of the α-hydroxy hydroperoxides compounds produced during the isoprene ozonolysis have been investigated in this paper. Geometrical parameters of all the stationary points as well as energies and rate constants have been computed by means of several ab initio and DFT methods (B3LYP, CCSD(T), and G2M-RCC5 levels). Our calculations indicate that only the water-assisted decomposition of the α-hydroxy hydroperoxides could be active in the atmosphere. The main reaction products are predicted to be H_2O_2 plus methyl vinyl ketone (**MVK**) or methacroleine (**MAC**), depending on the particular α-hydroxy hydroperoxide considered. In both cases the reaction is endothermic by about 19 kcal mol^{-1}.

Introduction

The gas-phase reaction of ozone with biogenic and anthropogenic olefins has received considerable attention because of the reported formation of OH radicals, H_2O_2, organic acids, and aldehydes into the atmosphere.[1−8] OH and H_2O_2 are among the most important oxidants in the atmosphere. Hydroxyl radical oxidizes many gaseous trace compounds, principally CO, CH_4, and nonmethane hydrocarbons. H_2O_2 is mainly responsible for the conversions of SO_2 into sulfuric acid (H_2SO_4).[9] Due to its high solubility it can deposit efficiently, both wet and dry, but also photolyze or react with OH. In the gas phase, it acts as a reservoir of atmospheric OH radicals.[10] Recent ice core records in Greenland show an increase of hydrogen peroxide, mainly over the past 20 years,[11] which enhances the atmospheric importance of this molecule. Consequences of increasing H_2O_2 are oxidative stress to vegetation[13] and possibly to people and animals. The mechanistic knowledge about its formation is therefore of great interest to explain atmospheric variations of this oxidant as well as to verify if the alkene ozonolysis represents an important source of H_2O_2 beside the recombination reaction of two HO_2 radicals.[13]

Isoprene (2-methylbuta-1,3-diene) is one of the most important nonmethane hydrocarbons in the atmosphere,[14] and its gas phase reaction with ozone represents an important atmospheric sink for this alkene. The general features of its mechanism are reasonably well established and are summarized in Scheme 1.

The reaction proceeds via the formation of the 1,2 and 3,4 primary ozonides, respectively. They decompose to produce carbonyl compounds and carbonyl oxides, which are also called Criegee intermediates (**CI**). These are methyl vinyl carbonyl oxide (**CI-a**, derived from 1,2-ozonide), isopropyl carbonyl oxide (**CI-b**, derived from 3,4-ozonide), and the parent H_2COO carbonyl oxide, derived from both 1,2- and 3,4-ozonides (see Scheme 1). These Criegee intermediates are formed with an excess of energy and can decompose unimolecularly. The decomposition mechanisms have been extensively investigated.[15,16] Moreover, Zhang et al.[16] have shown that an important fraction of **CI-a** and **CI-b** and almost all the H_2COO compound are vibrationally stabilized and may react with other atmospheric species such as water. The reaction of H_2COO with water as well as the formation and decomposition of HMHP have been reported in the literature [17] and will not be commented here. The reaction of **CI-a** and **CI-b** with water is reported in our previous paper.[18] Our calculations indicate that the α-hydroxy hydroperoxides **HP−I** and **HP−II** are almost exclusively formed as reaction products, although a small amount of **CI-a**, which possesses a syn-methyl hydrogen in the β-position with respect to the COO moiety, could produce OH radicals (see Scheme 1).

Very recently, Sauer et al.[8] pointed out that α-hydroxy hydroperoxides RR′C(OH)OOH formed during the reaction between carbonyl oxides and water may have different fates according to the nature of the R and R′ substitutes. The different possibilities have been summarized in eq 1.

$$H_2C(OH)OOH \rightarrow HCOOH + H_2O \quad (1a)$$

$$RHC(OH)OOH \rightarrow RHCO + H_2O_2 \quad (1b)$$

$$RHC(OH)OOH \rightarrow RC(O)OH + H_2O \quad (1c)$$

$$RR'C(OH)OOH \rightarrow RR'CO + H_2O_2 \quad (1d)$$

Recent theoretical studies of these processes on model systems[6,17] have also pointed out that the unimolecular decompositions described in eq 1 require very high activation enthalpies. However, the reaction between water and α-hydroxy hydroperoxides leads to the same products encountered during the unimolecular decomposition but requires smaller activation enthalpy. In this case, the water acts as a catalyst, which is regenerated at the end of the reaction. Following those theoretical studies, we have considered in this paper the unimolecular and water-assisted decomposition of the α-hydroxy hydroper-

* Corresponding author. E-mail: anglada@iiqab.csic.es.
† Institut d'Investigacions Químiques i Ambientals de Barcelona.
‡ Ecole Normale Supérieure de Lyon.

10.1021/jp034203w CCC: $25.00
Published on Web 07/08/2003

SCHEME 1

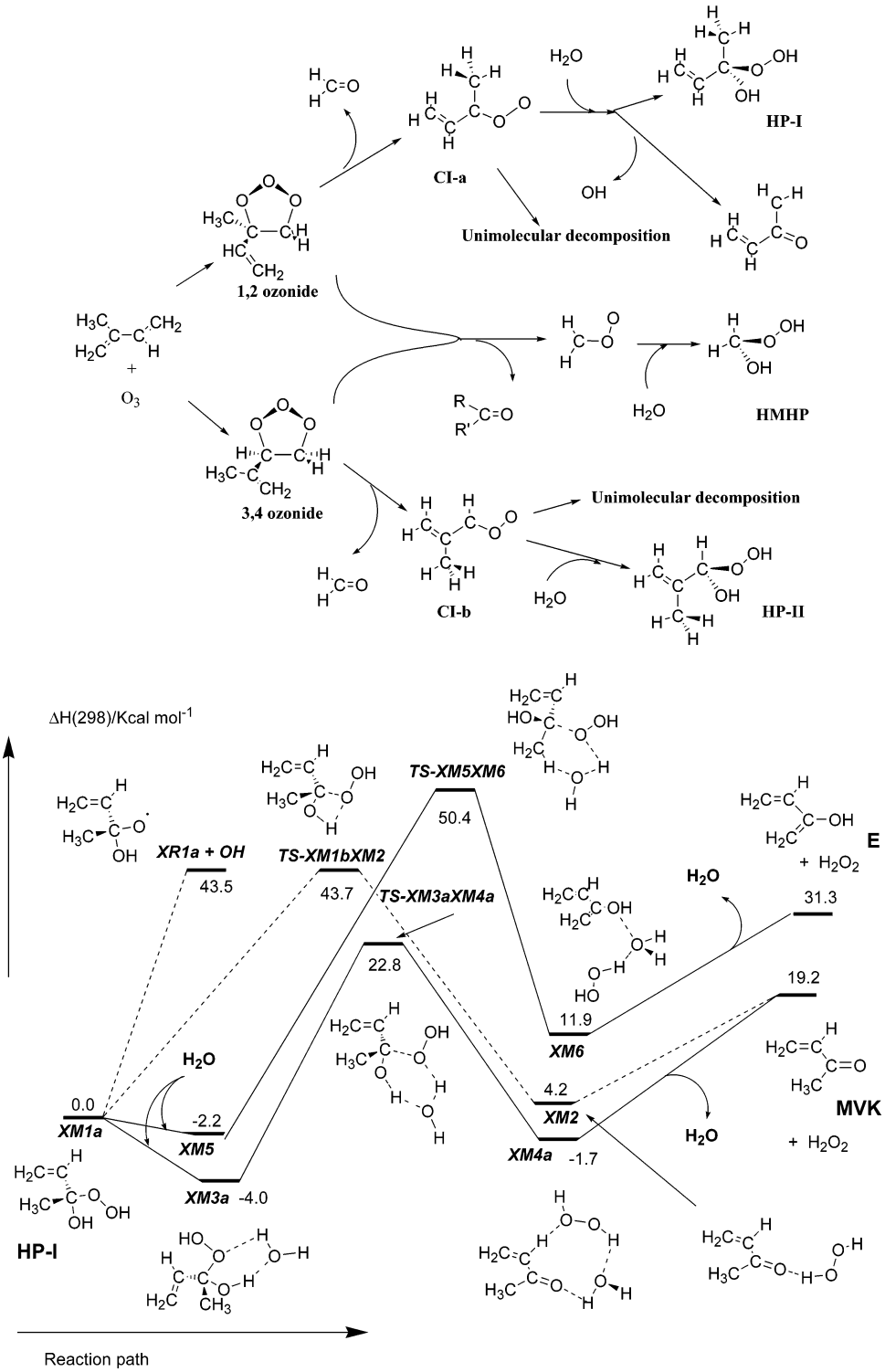

Figure 1. Schematic enthalpy diagram for the unimolecular (in dashed lines) and water-assisted (in solid lines) **HP−I** decomposition pathways. Enthalpies are computed at the G2M-RCC5 level of theory.

oxides **HP−I** and **HP−II** formed from the reaction of water with the different isoprene carbonyl oxides.

Computational Details

Geometry optimization of all the species considered in this study have been first carried out using DFT at the B3LYP/6-31G(d,p) level of theory.[19,20] At this level, harmonic vibrational frequencies have been calculated to verify the nature of the corresponding stationary point (minima or transition state) as well as to provide the zero point vibrational energy (ZPE) and the thermodynamic contributions to the enthalpy and the free energy. Moreover, to ensure that the transition states connect the desired reactants and products, intrinsic reaction coordinate calculations (IRC) have been performed for each transition state of every elementary reaction.

In a second step, all stationary points have been reoptimized using DFT with the more flexible 6-311+G(2d,2p) basis set, [21] which allows a better description of hydrogen-bond complexes

TABLE 1: Zero Point Energies (ZPE in kcal mol^{-1}), Entropies (*S* in eu) and Reaction and Activation Energies, Enthalpies, and Free Energies (*E*, *H*, and *G* in kcal mol^{-1}) for the Unimolecular and Water-Assisted Decomposition of HP-I[a,b]

compound	ZPE	S	relative to	E + ZPE	H_{298}	G_{298}
			Unimolecular Decomposition			
			(a) Formation of **MVK** + H_2O_2			
XM1a	75.8	85.6		0.0	0.0	0.0
XM1b	75.8	87.3	**XM1a**	1.5	1.6	1.1
TS-XM1bXM2	71.5	90.7	**XM1b**	41.7	42.0	41.0
XM2	74.5	99.5	**TS-XM1bXM2**	−40.2	−39.5	−42.1
MVK + H_2O_2	72.8	129.4	**XM2**	15.1	15.1	6.1
				(14.6)	(14.6)	(5.6)
			(b) Cleavage of the O−OH Bond			
XR1a + **Oh**[c]	70.1	12.1	**XM1a**	41.9	43.5	31.4
			Water-Assisted Decomposition			
			(a) Formation of **MVK** + H_2O_2 + H_2O			
XM1a + H_2O	90.0	132.0		0.0	0.0	0.0
XM1c + H_2O	89.1	132.2	**XM1a** + H_2O	2.3	2.5	2.0
XM3a	91.8	100.9	**XM1c** + H_2O	−6.4	−7.1	2.5
				(−5.8)	(−6.5)	(3.1)
TS-XM3aXM4a	87.5	96.3	**XM3a**	28.0	27.5	28.5
XM4a	90.1	117.1	**TS-XM3aXM4a**	−26.4	−24.6	−31.0
XM1d + H_2O	88.9	133.3	**XM1a** + H_2O	3.2	3.5	2.7
XM3b	91.7	100.5	**XM1d** + H_2O	−6.1	−6.9	2.9
				(−5.5)	(−6.3)	(3.5)
TS-XM3bXM4b	87.2	98.0	**XM3b**	27.8	27.3	28.1
XM4b	90.4	115.9	**TS-XM3bXM4b**	−27.5	−26.0	−31.3
MVK + H_2O_2 + H_2O	86.2	174.6	**XM4a**	20.5	20.9	4.0
				(19.5)	(19.9)	(3.0)
			(b) Formation of Enol (**E**) + H_2O_2 + H_2O			
XM1d + H_2O	88.9	133.3	**XM1a** + H_2O	3.2	3.5	2.7
XM5	91.7	102.3	**XM1d** + H_2O	−5.5	−6.2	−3.1
				(−5.0)	(−5.7)	(−2.6)
TS-XM5XM6	87.4	98.7	**XM5**	53.7	53.1	54.2
XM6	92.1	107.2	**TS-XM5XM6**	−39.5	−38.5	−41.1
E + H_2O_2 + H_2O	86.7	172.4	**XM6**	18.4	19.3	0.1
				(17.2)	(18.1)	(−1.1)

[a] The energies have been computed at the G2M-RCC5 level of theory. [b] **XM1** are isomers of **HP−I**. The energy values in parentheses are BSSE corrected. [c] These values are computed taking into account the CCSD(T)/6-311+G(2df,2p) energies as explained in ref 18.

and transition structures involving hydrogen transfer considered in this work. At this level of theory, basis set superposition errors (BSSE) have been corrected for all the hydrogen-bond complexes by the counterpoise method of Boys and Bernardi.[22]

In a third step, high-level single-point energy G2 (G2M-RCC5)[23] calculations have been performed on the B3LYP/6-311+G(2d,2p) geometries of all the stationary points in order to obtain more reliable energy values. The G2 (G2M-RCC5) model suggested by Mebel et al. requires RCCSD(T)/6-311G(d,p),[24] RMP2/6-311G(d,p),[25] and RMP2/6-311+G(3df,2p) single point calculations and includes "high level corrections" (HLC) based on the number of paired and unpaired electrons and zero point energy (ZPE) corrections.

Finally, rate constants for several elementary reactions of interest have been computed using classical transition-state theory. G2M-RCC5 and B3LYP/6-31G(d,p) partition functions and zero point corrections have been used. The tunneling corrections to the rate constants have been considered and computed by the zero-order approximation to the vibrationally adiabatic PES with zero curvature. The unsymmetrical Eckart potential energy barrier approximates the potential energy curve.[26]

All the geometry optimizations and the CCSD(T) calculations have been performed using the Gaussian 94[27] and Gaussian 98[28] suit of programs. The RCCSD(T) calculations over an ROHF wave function for the radicals have been done with the Molcas 4.1[29] program package and the kinetic results have been obtained with the TheRate program.[30]

Results and Discussion

Along the text, the structures of closed shell minima and radicals are designated by the letters **M** and **R**, respectively, and are followed by a number (**1**, **2**, and so on). To distinguish different isomers of a minimum, we have appended the small letters **a**, **b**, ... In addition, we have added the prefix **X** for the compounds derived from **HP−I** and the prefix **Y** for those derived from **HP−II**. Thus, for instance, **XM3a** and **XM3b** are different isomers of the same compound in the **HP−I** + H_2O reaction. The transition states are named by **TS** followed by the names of the two minima connected by them. In this paper we report only relative energies and some selected geometrical parameters. The Cartesian coordinates of all the structures as well as the absolute energies are available as Supporting Information.

(a) Decomposition of Methylvinyl α-Hydroxy Hydroperoxide (HP−I). In Figure 1 is presented a schematic G2M-RCC5 reaction enthalpy profile for the unimolecular and water-assisted decomposition of **HP−I**. The corresponding reaction and activation energies, enthalpies, and free energies are included in Table 1, while selected geometrical parameters of some representative stationary structures are displayed in Figure 2.

Methylvinyl α-hydroxy hydroperoxide (**HP−I**) has R and R′ ≠ H. According to eq 1d, we only expect the formation of methyl vinyl ketone (**MVK**) plus H_2O_2 from this compound. The different reaction paths involved in the unimolecular and water-assisted decomposition of **HP−I** begin with different conformers (**XM1a**, **XM1b**, **XM1c**, and **XM1d**, respectively),

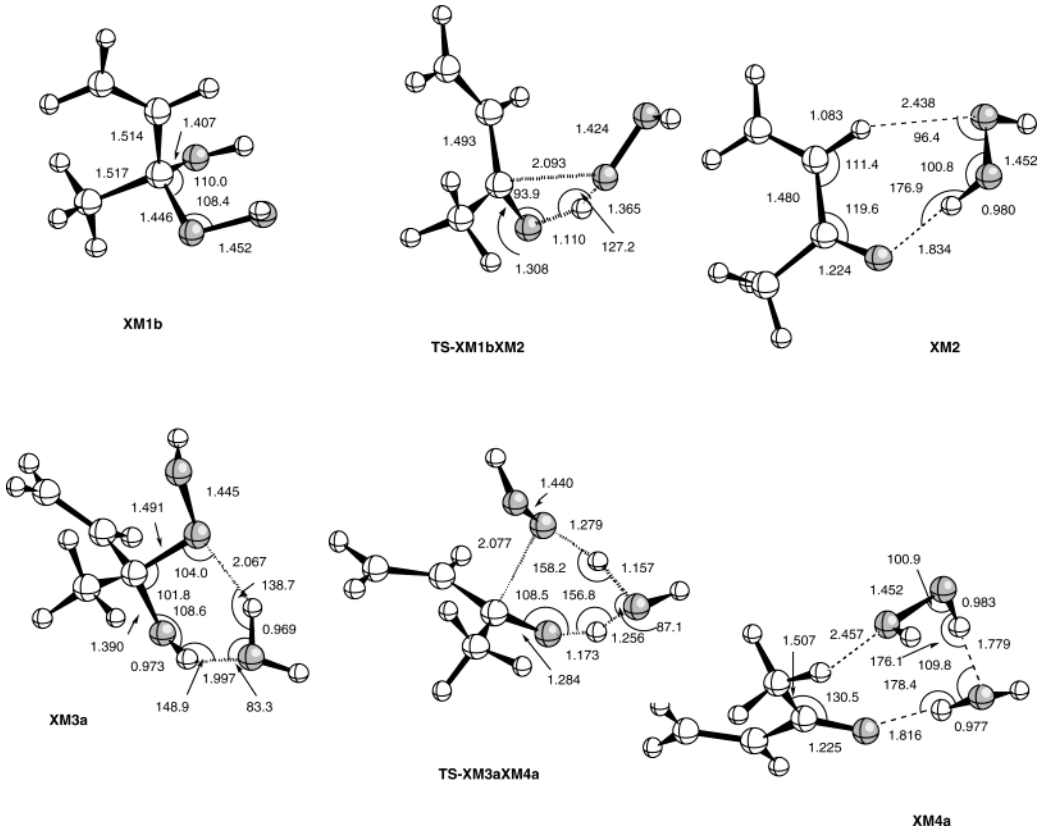

Figure 2. Selected B3LYP/6-311+G(2d,2p) geometrical parameters of some stationary points for the unimolecular and water-assisted **HP−I** decomposition pathways.

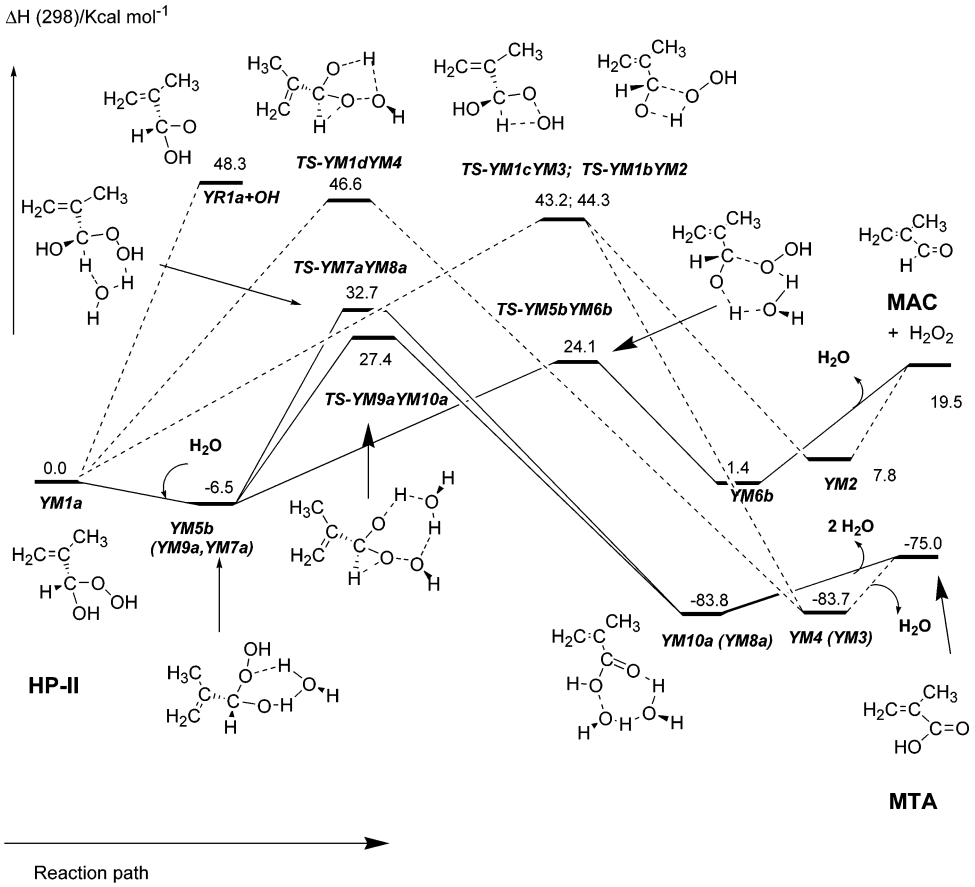

Figure 3. Schematic enthalpy diagram for the unimolecular (in dashed lines) and water-assisted (in solid lines) **HP−II** decomposition pathways. Enthalpies are computed at the G2M-RCC5 level of theory

TABLE 2: Zero Point Energies (ZPE in kcal mol^{-1}), Entropies (*S* in eu), and Reaction and Activation Energies, Enthalpies, and Free Energies (*E*, *H*, and *G* in kcal mol^{-1}) for the Unimolecular and Water-Assisted Decomposition of HP-ii[a,b]

compound	ZPE	S	relative to	E + ZPE	H_{298}	G_{298}
			Unimolecular Decomposition			
			(a) Formation of **MAC** + H_2O_2			
YM1a	76.5	86.9		0.0	0.0	0.0
YM1b	76.1	88.5	**YM1a**	1.3	1.4	1.0
TS-YM1bYM2	71.8	89.5	**YM1b**	42.8	42.9	42.6
YM2	74.3	100.5	**TS-YM1bYM2**	−37.6	−36.6	−39.9
MAC + H_2O_2	72.8	125.7	**YM2**	12.3	11.7	4.2
				(11.8)	(11.2)	(3.7)
			(b) Formation of ***syn-MTA*** + H_2O			
YM1c	76.1	89.3	**YM1a**	0.3	0.6	−0.2
TS-YM1cYM3	71.4	89.5	**YM1c**	42.5	42.6	42.5
YM3	75.3	97.5	**TS-YM1cYM3**	−121.6	−120.9	−123.2
syn-MTA + H_2O	73.5	123.8	**YM3**	2.5	2.6	−5.2
				(2.2)	(2.3)	(−5.5)
YM1d	76.2	87.8	**YM1a**	0.3	0.4	0.2
TS-YM1dYM4	71.0	86.2	**YM1d**	46.5	46.2	46.7
YM4	76.2	91.1	**TS-YM1dYM4**	−131.0	−130.3	−131.8
syn-MTA + H_2O	73.5	123.8	**YM4**	7.9	8.7	1.0
				(7.4)	(8.2)	(0.5)
			(c) Cleavage of the O-OH Bond			
YR1a + **OH**[c]	70.2	107.1	**YM1a**	39.5	41.2	29.2
			Water-Assisted Decomposition			
			(a) Formation of **MAC** + H_2O_2 + H_2O			
YM1a + H_2O	90.0	132.0		0.0	0.0	0.0
YM5a	92.0	102.9	**YM1a** + H_2O	−6.1	−6.5	2.2
				(−5.5)	(−5.9)	(2.8)
TS-YM5aYM6a	87.7	96.8	**YM5a**	33.8	33.1	34.9
YM6a	90.2	112.2	**TS-YM5aYM6a**	−26.9	−25.2	−29.8
YM1e + H_2O	89.9	135.8	**YM1a** + H_2O	3.1	3.5	2.3
YM5b	91.9	102.4	**YM1e** + H_2O	−5.5	−6.3	3.7
				(−4.9)	(−5.7)	(4.3)
TS-YM5bYM6b	87.6	97.9	**YM5b**	27.5	26.9	28.3
YM6b	90.3	114.4	**TS-YM5bYM6b**	−26.8	−25.3	−30.2
MAC + H_2O+ H_2O_2	86.2	170.8	**YM6a**	18.0	18.1	0.6
				(16.9)	(17.0)	(−0.5)
			(b) Formation of *syn*-MTA[d] + $2H_2O$			
YM7a	92.0	103.9	**YM1a** + H_2O	−3.7	−4.0	4.4
				(−3.2)	(−3.5)	(4.9)
TS-YM7aYM8a	87.4	96.8	**YM7a**	37.5	36.7	38.8
YM8a	91.2	111.0	**TS-YM7aYM8a**	−117.4	−115.8	−120.0
YM1f + H_2O	89.9	133.2	**YM1a** + H_2O	0.7	0.8	0.4
YM7b	91.3	108.3	**YM1f** + H_2O	−4.2	−4.3	3.1
				(−3.7)	(−3.8)	(3.6)
TS-YM7bYM8b	87.3	97.3	**YM7b**	39.2	38.0	41.0
YM8b	89.8	120.4	**TS-YM7bYM8b**	−119.2	−116.8	−123.5
syn-MTA + $2H_2O$	86.9	168.9	**YM8a**	7.2	8.0	−9.2
				(6.2)	(7.0)	(−10.2)
			(c) Formation of *anti*-MTA[d] + $2H_2O$			
YM1g + H_2O	89.3	133.7	**YM1a** + H_2O	2.0	2.2	1.7
YM9a	92.2	99.9	**YM1g** + H_2O	−5.7	−6.6	3.4
				(−5.1)	(−6.0)	(4.1)
TS-YM9aYM10a	86.6	95.9	**YM9a**	32.4	31.9	33.1
YM10a	91.6	108.1	**TS-YM9aYM10a**	−112.3	−111.0	−114.6
YM1h + H_2O	89.5	133.4	**YM1a** + H_2O	2.0	2.1	1.7
YM9b	91.2	103.4	**YM1h** + H_2O	−6.0	−6.4	2.5
				(−5.4)	(−5.8)	(3.1)
TS-YM9bYM10b			**YM9b**	33.5	32.8	34.4
YM10b	90.4	113.1	**TS-YM9bYM10b**	−112.8	−111.2	−115.7
***anti*-MTA** + $2H_2O$	86.6	169.3	**YM10a**	12.6	13.9	−4.4
				(11.3)	(12.6)	(−5.7)

[a] The energies have been computed at the G2M-RCC5 level of theory. [b] **YM1** are isomers of **HP**−**II**. The values in parenthesis are BSSE corrected. [c] These values are computed taking into account the CCSD(T)/6-311+G(2df,2p) energies as explained in ref 18. [d] **MTA** stands for methacrylic acid.

as indicated in Table 1, although they are not shown in Figure 1. The unimolecular process involves the isomer **XM1b**, the transition state **TS-XM1bXM2**, and the hydrogen-bond complex **XM2** before the formation of **MVK** plus H_2O_2. Figure 2 shows that the transition state is a four-membered ring in which simultaneously occur the cleavage of the CO bond of the hydroperoxide group (R(CO) = 2.093 Å), the migration of the hydrogen of the hydroxyl forming H_2O_2 (R(OH) = 1.110 Å and R(HO) = 1.365 Å), and the formation of the double bond of the carbonyl group (compare the R(CO) = 1.308 Å in **TS-XM1bXM2** with the corresponding value of 1.407 Å in **XM1b**). The computed activation enthalpy is 42 kcal mol^{-1}. It is about the same energy required for the cleavage of the OO bond in **XM1a** to produce **XR1a** + OH (see Figure 1). However, in

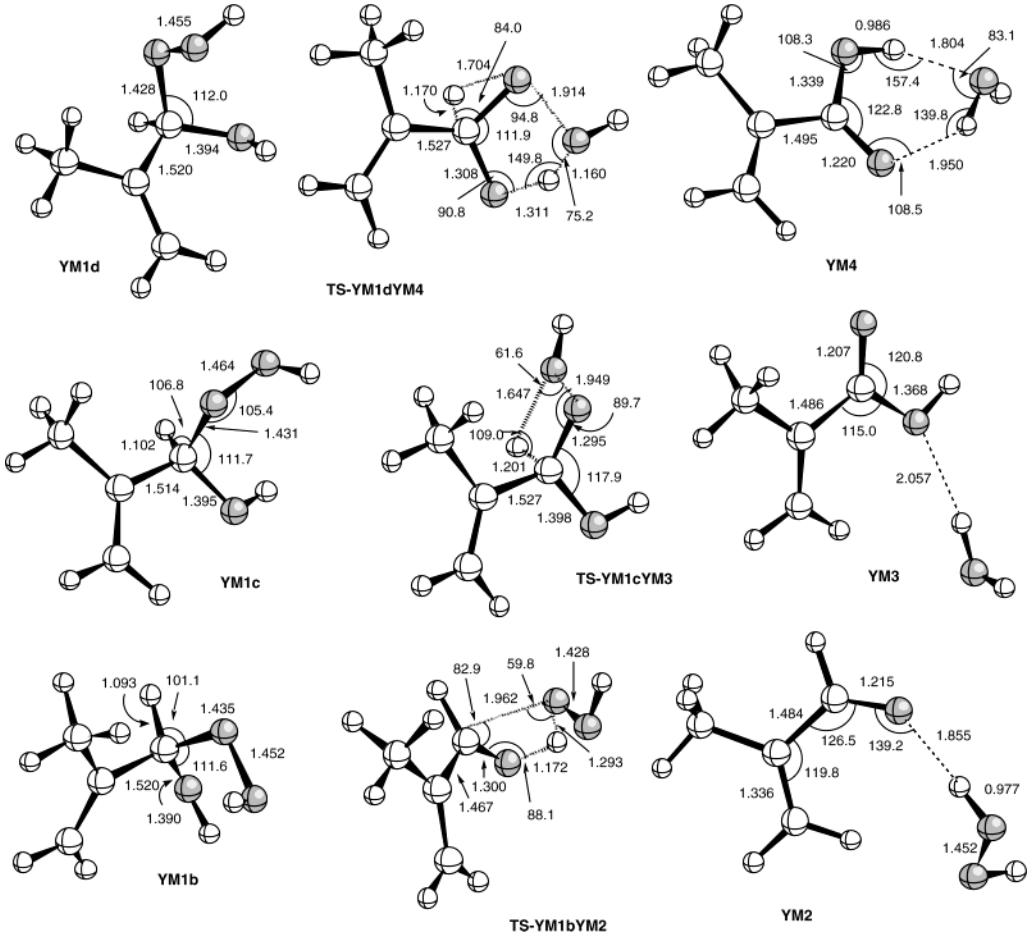

Figure 4. Selected B3LYP/6-311+G(2d,2p) geometrical parameters of the stationary points for the unimolecular **HP−II** decomposition pathways.

our previous paper,[18] we have already pointed out that methylvinyl α-hydroxy hydroperoxide (**HP−I**) is formed with a lesser excess of energy (about 38 kcal mol^{-1}), and consequently, we expect that these unimolecular processes would not occur.

For the bimolecular reaction of **HP−I** with water, producing **MVK** + H_2O_2 + H_2O, we have considered two different reaction paths involving the cis and trans isomers with respect to the methyl and vinyl groups. For each path, the reaction begins with the formation of a hydrogen-bond complex (**XM3a** or **XM3b**) between an isomer of **HP−I** and H_2O. In the first path considered, this complex evolves to another hydrogen-bond complex (**XM4a** or **XM4b**) via a six-membered ring transition state (**TS-XM3aXM4a** or **TS-XM3bXM4b**). The **XM4** complexes are formed with the three fragments **MVK**, H_2O, and H_2O_2 corresponding to the products of the reaction. Comparison of **TS-XM3aXM4a** and **TS-XM1bXM2** structures displayed in Figure 2 clearly shows that the unimolecular and water-assisted processes are essentially the same. However, the water molecule facilitates the transfer of the hydrogen atoms in the bimolecular one. Let us compare the four-membered ring of the unimolecular reaction with the six-membered ring in the water-assisted process in Figure 2. The bimolecular formation of **MVK** from **HP−I** is endoergic by 19.2 kcal mol^{-1} with respect to the most stable isomer **XM1a** and requires an activation enthalpy of about 27.5 kcal mol^{-1} (**TS-XM3aXM4a** relative to **XM3a**, or **TS-XM3bXM4b** relative to **XM3b**; see Table 1). The activation enthalpy is about 15 kcal mol^{-1} smaller than the one encountered for the unimolecular process (**TS-XM1bXM2** in Table 1), which can be associated with the catalytic effect of water. It is also interesting to point out the large stability computed for the hydrogen-bond complexes **XM4a** and **XM4b**, which are about 20 kcal mol^{-1} more stable than the **MVK**, H_2O, and H_2O_2 products.

For a shake of completeness we have also considered another possible reaction involving the water-assisted abstraction of one hydrogen from the methyl group in the methylvinyl α-hydroxy hydroperoxide compound. The fate of this process is 2-hydroxy-1,3-butadiene (**E**) plus H_2O_2. This reaction requires a very large activation enthalpy (53.1 kcal mol^{-1} for **TS-XM5XM6**; see Table 1 and Figure 1), which makes this process unlikely.

(b) Decomposition of 2-Propenyl α-Hydroxy Hydroperoxide (HP−II). In Figure 3 is presented a schematic G2M-RCC5 reaction enthalpy profile for the unimolecular and water-assisted decomposition of **HP−II**. The corresponding reaction and activation energies, enthalpies, and free energies are included in Table 2, while the most relevant geometrical parameters of some selected stationary points are displayed in Figures 4 and 5. In the 2-propenyl α-hydroxy hydroperoxide, a substitute is a hydrogen atom and, according to eqs 3b and 3c, the fate of its decomposition could be methacrolein (**MAC**) plus H_2O_2 and methacrylic acid (**MTA**) plus H_2O. An important point here is to predict which product is formed and to what extent.

For the unimolecular decomposition of **HP−II**, we have found two reaction paths yielding **MTA** + H_2O (via **TS-YM1dYM4** and **TS-YM1cYM3**, respectively) and one reaction path producing **MAC** + H_2O_2 (via **TS-YM1bYM2**). In addition, the cleavage of the O−OH bond producing **YR1a** + OH is also envisageable (see Figure 3 and our previous paper[18]). All the transition structures relative to these processes have been displayed in Figure 4. They essentially show the same features

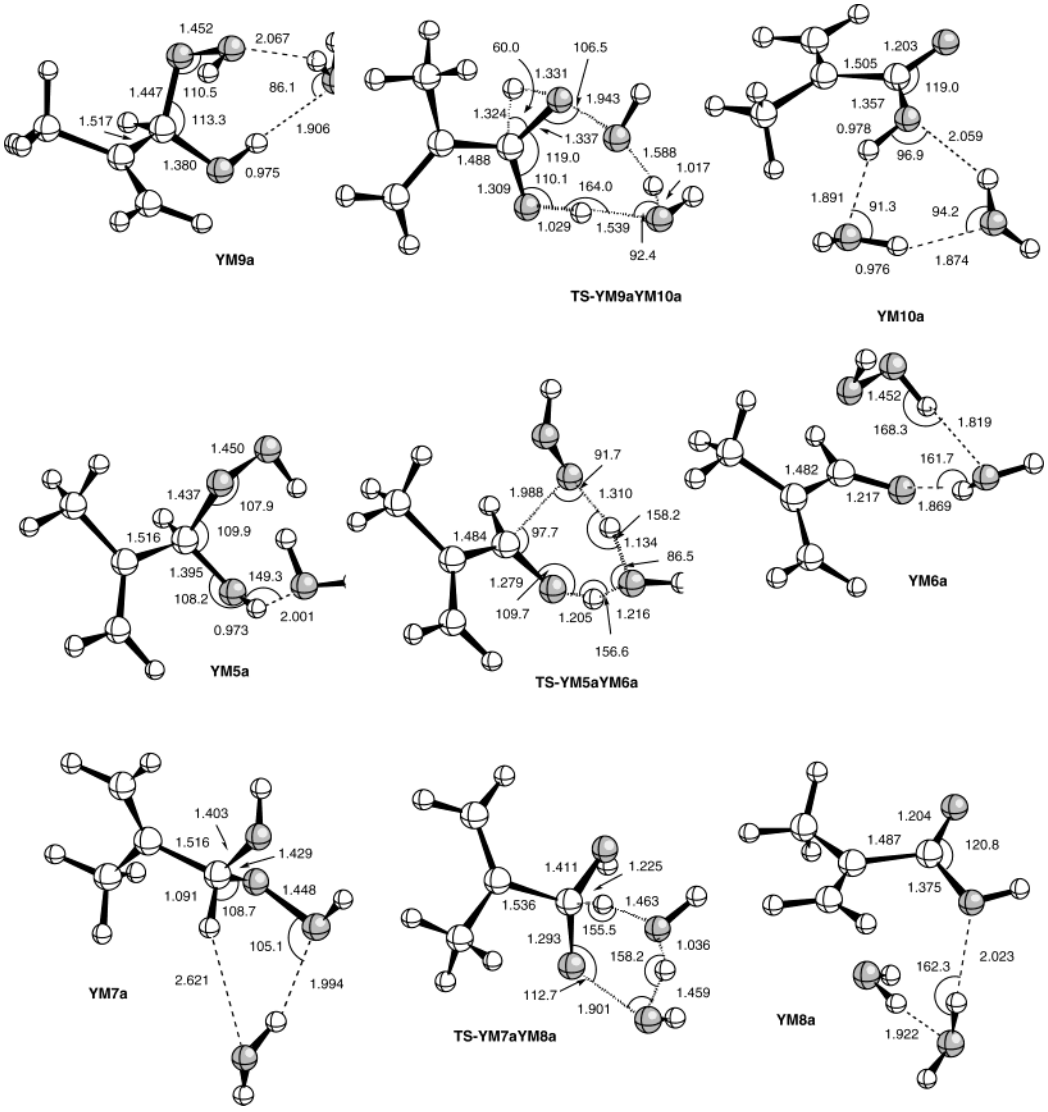

Figure 5. Selected B3LYP/6-311+G(2d,2p) geometrical parameters for some of the stationary points of the water-assisted **HP**−**II** decomposition pathways.

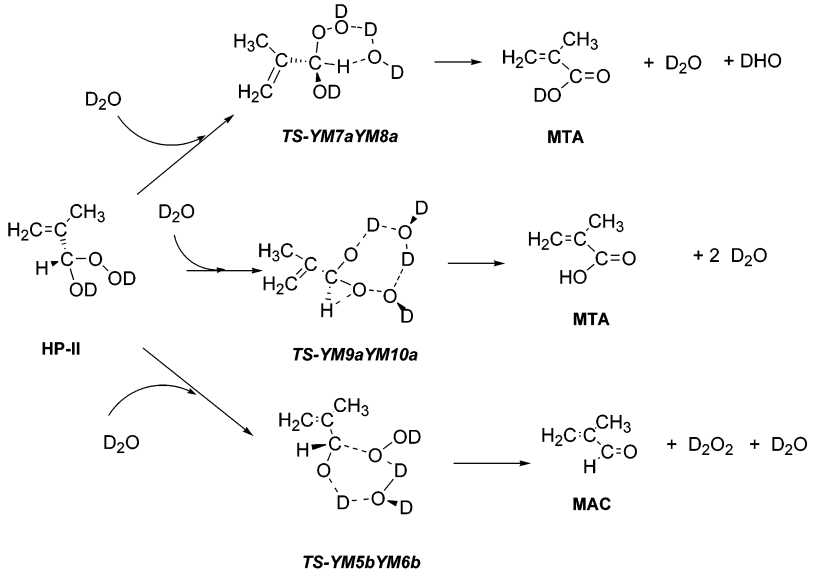

Figure 6. Schematic reaction mechanism of the reaction between deuterated **HP**−**II** and D_2O.

discussed in the literature.[6,17] Table 2 indicates that the activation enthalpies for all the unimolecular processes lie between 42 and 46 kcal mol^{-1}. These values are larger than the excess of energy released in the formation of **HP**−**II** (see the preceding paper). It is therefore expected that these unimolecular decomposition pathways would not be active under atmospheric conditions.

TABLE 3: Calculated Tunneling Parameters, κ, and Rate Constants, k (s^{-1}), for the Water-Assisted Decomposition of HP-II at 298.15 K[a]

	TS-YM5aYM6a	TS-YM5bYM6b	TS-YM7aYM8a	TS-YM7bYM8b	TS-YM9aYM10a	TS-YM9bYM10b
κ	8.446	8.754	2.861	1.769	4.080	4.324
k_i	1.3585×10^{-12}	1.0417×10^{-7}	6.3540×10^{-16}	8.6864×10^{-18}	1.700×10^{-11}	1.5401×10^{-12}
$\Gamma = k_i/\kappa^b$		99.98			0.02	

[a] The partition functions have been calculated at the B3LYP/6-31G(d,p) level of theory and the energies at the G2M-RCC5 level of theory. [b] $k = \sum_i k_i$ is the total rate constant and $\Gamma = k_i/\kappa$ corresponds to the branching ratio (in percent) for each process.

For the bimolecular reaction between **HP−II** and water, the cis and trans isomers with respect to the 2-propenyl group have been considered. Six different reaction paths have been found, four producing **MTA** plus H_2O and two yielding **MAC** plus H_2O_2. In all cases, the catalytic water molecule is regenerated at the end of the reaction. The structures of only one isomer of **MTA** and **MAC** have been displayed in Figure 5.

All the bimolecular reactions begin with the formation of a hydrogen-bond complex between **HP−II** and H_2O. They involve a second H bond complex just before the formation of the products, **MTA** + $2H_2O$ and **MAC** + H_2O_2 + H_2O, respectively. As for **HP−I**, the structures of the water-assisted transition states (see Figures 3 and 5) clearly show the same features as the corresponding transition state of the unimolecular decomposition pathways (compare **TS-YM1dYM4** with **TS-YM9aYM10a**, **TS-YM1cYM3** with **TS-YM7aYM8a,** and **TS-YM1bYM2** with **TS-YM5aYM6a** in Figures 4 and 5). However, the water molecule acts as a catalyst and facilitates the transfer of the hydrogen atoms in bimolecular reactions. The energetic values gathered in Table 2 and reported in Figure 3 indicate that the initial hydrogen-bond complexes are about 6 kcal mol^{-1} more stable than the corresponding reactants, whereas the outgoing hydrogen-bond complexes are between 10 and 12 kcal mol^{-1} more stable than the products. In addition, it can be seen that the formation of **MAC** + H_2O_2 is endothermic by about 19 kcal mol^{-1}. On the other hand, the formation of **MTA** + H_2O is exothermic by about 75 kcal mol^{-1} (relative to the most stable isomer **YM1a** of **HP−II**). Regarding the activation enthalpies, Table 2 shows that the most favorable process is the formation of **MAC** + H_2O_2 + H_2O via **TS-YM5bYM6b**, with a computed activation enthalpy of 26.9 kcal mol^{-1}. The reaction that involves the other isomer (via **TS-YM5aYM6a**) has a larger activation enthalpy (33.1 kcal mol^{-1}). In addition, the corresponding barriers for the formation of **MTA** plus H_2O (via **TS-YM9aYM10a**; **TS-YM9bYM10b**; **TS-YM7aYM8a** and **TS-YM7bYM8b**) range from 32 to 38 kcal mol^{-1}. Thus, these results suggest that **MAC** + H_2O_2 + H_2O will be the product formed principally, despite the reaction being endothermic. Furthermore, it is also worth pointing out that the catalytic effect of water in the **HP−II** decomposition processes lies between 10 and 15 kcal mol^{-1} (see Table 2).

The results of the mechanistic study carried out in the present work show that the different reaction paths of the water-assisted **HP−II** decomposition are clearly distinguishable by performing experiments with D_2O instead H_2O, and accordingly, we have schematized in Figure 6 the fates of the different reaction paths in such hypothetical experiments with deuterated water. In the previous paper[18] we have pointed out that isoprene ozonolysis with D_2O will produce **HP−II** with deuterated hydroxyl and hydroperoxyl groups, as shown in Figure 6. Then, the further reaction of this deuterated **HP−II** with D_2O will yield deuterated **MTA** plus DHO, if reaction takes place through **TS-YM7aYM8a**, nondeuterated **MTA** if the reaction takes place through **TS-YM9aYM10a**, and D_2O_2 in the reaction path leading to the formation of **MAC** (via **TS-YM5bYM6b**)

Finally, to estimate the competition between the reactions between water and **HP−II** producing **MAC** + H_2O_2 and **MTA** + H_2O, respectively, the unimolecular rate constants have been computed using the classical transition state theory. The corresponding branching ratios for these processes are showed in Table 3. Our values show that practically only the **TS-YM5bYM6b** channel, producing **MAC** + H_2O_2 + H_2O, is active, and therefore, these results lead to the conclusion that the reaction of **HP−II** with water is given by eq 2.

$$\text{HP-II} + \text{H}_2\text{O} \underset{k_{-1}}{\overset{k_1}{\rightleftharpoons}} \text{HP-II}\cdots\text{H}_2\text{O} \xrightarrow{k_2} \text{MAC} + \text{H}_2\text{O}_2 + \text{H}_2\text{O} \tag{2}$$

Here, according to the elementary processes described above, **HP−II** corresponds to **YM1e**, the HP−II···H_2O is the hydrogen-bond complex **YM5b**, and the transition state connecting this complex with the products corresponds to **TS-YM5bYM6b**. At this point it is interesting to provide an estimate of the rate coefficient of this reaction. Our calculated entropy values and free energy differences displayed in Table 2 show that the complex **YM5b** is highly shifted to the reactants, and upon applying steady state theory, the whole rate constant is given by eq 3.

$$k = \frac{k_1}{k_{-1}} k_2 = K_{eq} k_2 \tag{3}$$

According to transition state theory, the equilibrium constant K_{eq} and the rate constant k_2 of the second step are given by eqs 4 and 5 respectively

$$K_{eq} = \frac{Q_{YM5b}}{Q_{YM1e} Q_{H_2O}} e^{-(E_C - E_R)/RT} \tag{4}$$

$$k_2 = \kappa \frac{k_b T}{h} \frac{Q_{TS}}{Q_{YM5b}} e^{-(E_{TS} - E_C)/RT} \tag{5}$$

where the various Q denote the partition functions of the reactants **YM1e** and H_2O, the hydrogen-bond complex **YM5b**, and the transition state **TS-YM5bYM6b**; E_R, E_C, and E_{TS} are the total energies of the reactants, hydrogen-bond complex, and transition state, respectively; k_b and h are the Boltzmann and Planck constants, respectively; and κ is the tunneling parameter contained in Table 3. Then, the computed rate constant for the overall reaction 2 is given by eq 6.

$$k = \kappa \frac{k_b T}{h} \frac{Q_{TS}}{Q_{YM1e} Q_{H_2O}} e^{-(E_{TS} - E_R)/RT} \tag{6}$$

Here, $(E_{TS} - E_R) = 22.6$ kcal mol^{-1}, which includes the ZPE

energy and the BSSE correction (see Table 2), and k is calculated to be 1.4967×10^{-30} cm^3 molecule^{-1} s^{-1}.

Conclusions

In this paper, a theoretical investigation on the unimolecular and water-assisted decomposition of the α-hydroxy hydroperoxydes **HP−I** and **HP−II** has been reported. These two compounds are formed during isoprene ozonolysis.[18] The results of the present study lead to the following conclusions that are of interest in atmospheric chemistry.

(1) The unimolecular decomposition of both **HP−I** and **HP−II** requires very high activation enthalpies (about 44 kcal mol^{-1}). This value is larger than the energy released during the formation of these two species by the reaction of isoprene carbonyl oxides with water.[18] We therefore predict that the unimolecular decomposition of **HP−I** and **HP−II** would not be active in the atmosphere.

(2) The α-hydroxy hydroperoxides **HP−I** and **HP−II** can react with a water molecule, which acts as a catalyst, to produce the same species as those found for the unimolecular decomposition pathway. The reaction between **HP−I** and H_2O produces **MVK** + H_2O_2 exclusively. The reaction between **HP−II** and H_2O has two possible fates, **MAC** + H_2O_2 and **MTA** + H_2O, respectively, and in this case, experiments with D_2O are proposed that allow clear identification of the different reaction mechanisms considered. The activation enthalpies and the computed unimolecular reaction constants indicate that the reaction between **HP−II** and water yields almost exclusively **MAC** + H_2O_2. In this case, the calculated rate constant is 1.4967×10^{-30} cm^3 molecule^{-1} s^{-1}.

Acknowledgment. The financial support for this work was provided by the Dirección General de Investigación Científica y Técnica (DGICYT, Grant BQU2002-0485-C02-01) and by the Generalitat de Catalunya (Grant 2001SGR00048). P.A. thanks the European Community—Access to Research Infrastructure Action of the Improving Human Potential Program—for financial support. The calculations described in this work were performed at the Centre de Supercomputació de Catalunya (CESCA), whose services are gratefully acknowledged.

Supporting Information Available: The Cartesian coordinates and absolute energies of all stationary points reported in this paper. This material is available free of charge via the Internet at http://pubs.acs.org.

References and Notes

(1) (a) Kroll, J. H.; Donahue, N. M.; Cee, V. J.; Demerjian, K. L.; Anderson, J. G. *J. Am. Chem Soc.* **2002**, *124*, 8518. (b) Kroll, J. H.; Hanisco, T. F.; Donahue, N. M.; Demerjian, K. L.; Anderson, J. G. *Geophys. Res. Lett.* **2001**, *28*, 3863. (c) Kroll, J. H.; Sahay, S. R.; Anderson, J. G.; Donahue, N. M.; Demerjian, K. L. *J. Phys. Chem. A* **2001**, *105*, 4446. (d) Donahue, N. M.; Kroll, J. H.; Anderson, J. G.; Demerjian, K. L. *Geophys. Res. Lett.* **1998**, *25*, 59.

(2) (a) Orzechowska, G. E.; Paulson, S. E. *Atmos. Environ.* **2002**, *36*, 571. (b) Fenske, J. D.; Kuwata, K. T.; Houk, K. N.; Paulson, S. E. *J. Phys. Chem. A* **2000**, *104*, 7246. (c) Fenske, J. D.; Hasson, A. S.; Paulson, S. E.; Kuwata, K. T.; Ho, A.; Houk, K. N. *J. Phys. Chem. A* **2000**, *104*, 7821. (d) Paulson, S. E.; Chung, M. T.; Hasson, A. *J. Phys. Chem. A* **1999**, *103*, 8125. (e) Paulson, S. E.; Orlando, J. J. *Geophys. Res. Lett.* **1996**, *23*, 3727.

(3) (a) Rickard, A. R.; Johnson, D.; McGill, C. D.; Marston, G. *J. Phys. Chem. A* **1999**, *103*, 7656. (b) McGill, C. D.; Rickard, A. R.; Johnson, D.; Marston, G. *Chemosphere* **1999**, *38*, 1205. (c) Schäfer, C.; Horie, O.; Crowley, J. N.; Moortgat, G. K. *Geophys. Res. Lett.* **1997**, *24*, 1611. (d) Atkinson, R.; Aschmann, S. M. *Environ. Sci. Technol.* **1993**, *27*, 1357.

(4) (a) Johnson, D.; Lewin, A. G.; Marston, G. *J. Phys. Chem. A* **2001**, *105*, 2933. (b) Neeb, P.; Moortgat, G. K. *J. Phys. Chem. A* **1999**, *103*, 9003.

(5) (a) Kroll, J. H.; Clarke, J. S.; Donahue, N. M.; Anderson, J. G.; Demerjian, K. L. *J. Phys. Chem. A* **2001**, *105*, 1554. (b) Niki, H.; Maker, P. D.; Savage, C. M.; Breitenbach, L. P.; Hurley, M. D. *J. Phys. Chem.* **1987**, *91*, 941.

(6) Anglada, J. M.; Aplincourt, P.; Bofill, J. M.; Cremer, D. *Chem. Phys. Chem.* **2002**, *2*, 215.

(7) (a) Moortgat, G. K.; Grossmann, D.; Boddenberg, A.; Dallmann, G.; Ligon, A. P.; Turner, W. V.; Gäb, S.; Slemr, F.; Wieprecht, W.; Acker, K.; Kibler, M.; Schlomski, S.; Bächmann, K. *J. Atmos. Chem.* **2002**, *42*, 443. (b) Becker, K. H.; Bechara, J.; Brockmann, K. J. *Atmos. Environ.* **1993**, *27A*, 57. (c) Becker, K. H.; Brockmann, K. J.; Bechara, J. *Nature* **1990**, *346*, 256.

(8) Sauer, F.; Schäfer, C.; Neeb, P.; Horie, O.; Moortgat, G. K. *Atmos. Environ.* **1999**, *33*, 229.

(9) Hoffman, M. R.; Edwards, J. O. *J. Phys. Chem.* **1975**, *79*, 2096.

(10) (a) Crutzen, P. J.; Lawrence, M. L.; Pöschl, U. *Tellus* **1999**, *51A−B*, 123. (b) Jackson, A. V.; Hewitta, C. N. *Crit. Rev. Environ. Sci. Technol.* **1995**, *29*, 175.

(11) (a) Sigg, A.; Neftel, A. *Nature* **1991**, *351*, 557. (b) Anklin, M.; Bales, R. C. *J. Geophys. Res.* **1997**, *102*, 19099.

(12) Möller, D. *Atmos. Environ.* **1989**, *23*, 1625.

(13) Calvert, J. G.; Stockwell, W. R. *Environ. Sci. Technol.* **1983**, *17*, 428.

(14) Warnecke, C.; Holzinger, R.; Hansel, A.; Jordan, A.; Lindinger, W.; Pöschl, U.; Williams, J.; Hoor, P.; Fischer, H.; Crutzen, P. J.; Scheeren, H. A.; Lelieveld, J. *J. Atmos. Chem.* **2001**, *38*, 167.

(15) (a) Niki, H.; Maker, P. D.; Savage, C. M.; Breitenbach, L. P.; Hurley, M. D. *J. Phys. Chem.* **1987**, *91*, 941.(b) Martinez, R. I.; Herron, J. T. *J. Phys. Chem.* **1987**, *91*, 946. (c) Neeb, P.; Horie, O.; Moortgat, G. K. *J. Phys. Chem. A* **1998**, *102*, 6778. (d) Herron, J. T.; Huie, E. *J. Am. Chem. Soc.* **1977**, *99*, 5430. (e) Martinez, R. I.; Herron, J. T. *J. Phys. Chem.* **1988**, *92*, 4644. (f) Gutbrod, R.; Kraka, E.; Schindler, R. N.; Cremer, D. *J. Am. Chem. Soc.* **1997**, *119*, 7330. (g) Anglada, J. M.; Bofill, J. M.; Olivella, S.; Solé, A. *J. Phys. Chem. A* **1998**, *19*, 3398. (h) Chen, B. Z.; Anglada, J. M.; Huang, M. B.; Kong, F. *J. Phys. Chem. A* **2002**, *106*, 1877. (i) Paulson, S. E.; Chung, M. Y.; Hasson, A. S. *J. Phys. Chem. A* **1999**, *103*, 8127.

(16) (a) Zhang, D.; Zhang, R. *J. Am. Chem. Soc*. **2002**, *124*, 2692. (b) Zhang, D.; Zhang, R. *Chem. Phys. Lett.* **2002**, *358*, 171

(17) Crehuet, R.; Anglada, J. M.; Bofill, J. M. *Chem. Eur. J.* **2001**, *7*, 2227.

(18) Aplincourt, P.; Anglada, J. M. *J. Phys. Chem. A* **2003**, *107*, 5798 (preceding paper in this issue).

(19) Becke, A. D. *J. Chem. Phys.* **1993**, *98*, 5648.

(20) Hariharan, P. C.; Pople, J. A. *Theor. Chim. Acta* **1973**, *28*, 213.

(21) Krishnan, R.; Binkley, J. S.; Seeger, R.; Pople, J. A. *J. Chem. Phys.* **1980**, *72*, 650.

(22) Boys, S. F.; Bernardi, F. *Mol. Phys.* **1970**, *19*, 553.

(23) Mebel, A. M.; Morokuma, K.; Lin, M. C. *J. Chem. Phys.* **1995**, *103*, 7414.

(24) (a) Cizek, J. *Adv. Chem. Phys.* **1969**, *14*, 35. (b) Barlett, R. J. *J. Phys. Chem.* **1989**, *93*, 1963. (c) Raghavachari, K.; Trucks, G. W.; Pople, J. A.; Head-Gordon, M. *Chem. Phys. Lett.* **1989**, *157*, 479.

(25) (a) Møller, C.; Plesset, M. S. *Phys. Rev.* **1934**, *46*, 618. (b) Pople, J. A.; Binkley, J. S.; Seeger, R. *Int. J. Quantum Chem. Symp.* **1980**, *10*, 1. (c) Krishnan, R.; Pople, J. A. *Int. J. Quantum Chem.* **1978**, *14*, 91. (d) Krishnan, R.; Frisch, M. J.; Pople, J. A. *J. Chem. Phys.* **1980**, *72*, 4244.

(26) Truong, T. N.; Truhlar, D. G. *J. Chem. Phys.* **1990**, *93*, 1761.

(27) Frisch, M. J.; Trucks, G. W.; Schlegel, H. B.; Gill, P. M. W.; Johnson, B. G.; Robb, M. A.; Cheeseman, J. R.; Keith, T.; Petersson, G. A.; Montgomery, J. A.; Raghavachari, K.; Al-Laham, M. A.; Zakrzewski, V. G.; Ortiz, J. V.; Foresman, J. B.; Peng, C. Y.; Ayala, P. Y.; Chen, W.; Wong, M. W.; Andres, J. L.; Replogle, E. S.; Gomperts, R.; Martin, R. L.; Fox, D. J.; Binkley, J. S.; Defrees, D. J.; Baker, J.; Stewart, J. P.; Head-Gordon, M.; Gonzalez, C.; Pople, J. A. *Gaussian 94*, Revision B.3; Gaussian Inc.: Pittsburgh, PA, 1995.

(28) Frisch, M. J.; Trucks, G. W.; Schlegel, H. B.; Scuseria, G. E.; Robb, M. A.; Cheeseman, J. R.; Zakrzewski, V. G.; Montgomery, J. A.; Stratmann, R. E.; Burant, J. C.; Dapprich, S.; Millam, J. M.; Daniels, A. D.; Kudin, K. N.; Strain, M. C.; Farkas, O.; Tomasi, J.; Barone, V.; Cossi, M.; Cammi, R.; Mennucci, B.; Pomelli, C.; Adamo, C.; Clifford, S.; Ochterski, J.; Petersson, G. A.; Ayala, P. Y.; Cui, Q.; Morokuma, K.; Malick, D. K.; Rabuck, A. D.; Raghavachari, K.; Foresman, J. B.; Cioslowski, J.; Ortiz, J. V.; Stefanov, B. B.; Liu, G.; Liashenko, A.; Piskorz, P.; Komaromi, I.; Gomperts, R.; Martin, R. L.; Fox, D. J.; Keith, T.; Al-Laham, M. A.; Peng, C. Y.; Nanayakkara, A.; Gonzalez, C.; Challacombe, M.; Gill, P. M. W.; Johnson, B. G.; Chen, W.; Wong, M. W.; Andres, J. L.; Head-Gordon, M.; Replogle, E. S.; Pople, J. A. *Gaussian 98*, Revision A.5; Gaussian, Inc.: Pittsburgh, PA, 1998.

(29) Andersson, K.; Blomberg, M. R. A.; Fülscher, M. P.; Karlstrom, G.; Lindh, R.; Malmqvist, P.; Neogrady, P.; Olsen, J.; Roos, B. O.; Sadlej, A. J.; Schutz, M.; Seijo, L.; Serrano-Andres, L.; Siegbahn, P. E. M.; Widmark, P. O. *MOLCAS*, Version 4.1; Lund University: Sweden, 1998.

(30) Duncan, W. T.; Truong, T. N. http://therate.hec.utah.edu (accessed September 2000).